DNA-TR-88-180

VANE FLOW DIRECTION SENSOR FOR BLAST WAVES

N. H. Ethridge
G. T. Watson
Tech. Reps., Inc.
Aberdeen Research Center
P. O. Box 548
Aberdeen, MD 21001

7 February 1987

Technical Report

CONTRACT No. DNA 001-86-C-0249

Approved for public release;
distribution is unlimited.

THIS WORK WAS SPONSORED BY THE DEFENSE NUCLEAR AGENCY
UNDER RDT&E RMC CODE B3100864662 RW RA 00037 25904D.

Prepared for
Director
Defense Nuclear Agency
Washington, DC 20305-1000

Destroy this report when it is no longer needed. Do not return to sender.

PLEASE NOTIFY THE DEFENSE NUCLEAR AGENCY, ATTN: CSTI, WASHINGTON, DC 20305-1000, IF YOUR ADDRESS IS INCORRECT, IF YOU WISH IT DELETED FROM THE DISTRIBUTION LIST, OR IF THE ADDRESSEE IS NO LONGER EMPLOYED BY YOUR ORGANIZATION.

DISTRIBUTION LIST UPDATE

This mailer is provided to enable DNA to maintain current distribution lists for reports. We would appreciate your providing the requested information.

☐ Add the individual listed to your distribution list.

☐ Delete the cited organization/individual.

☐ Change of address.

NAME: _____

ORGANIZATION: _____

OLD ADDRESS	CURRENT ADDRESS
_____	_____
_____	_____
_____	_____

TELEPHONE NUMBER: ( ) _____

SUBJECT AREA(s) OF INTEREST:

_____	_____
_____	_____
_____	_____

DNA OR OTHER GOVERNMENT CONTRACT NUMBER: _____

CERTIFICATION OF NEED-TO-KNOW BY GOVERNMENT SPONSOR (if other than DNA):

SPONSORING ORGANIZATION: _____

CONTRACTING OFFICER OR REPRESENTATIVE: _____

SIGNATURE: _____

CUT HERE AND RETURN

UNCLASSIFIED
SECURITY CLASSIFICATION OF THIS PAGE

REPORT DOCUMENTATION PAGE

1a REPORT SECURITY CLASSIFICATION UNCLASSIFIED	1b RESTRICTIVE MARKINGS
2a SECURITY CLASSIFICATION AUTHORITY N/A since Unclassified	3 DISTRIBUTION/AVAILABILITY OF REPORT Approved for public release; distribution is unlimited.
2b DECLASSIFICATION/DOWNGRADING SCHEDULE N/A since Unclassified	
4 PERFORMING ORGANIZATION REPORT NUMBER(S)	5 MONITORING ORGANIZATION REPORT NUMBER(S) DNA-TR-88-180
6a NAME OF PERFORMING ORGANIZATION Tech. Reps., Inc. Aberdeen Research Center 6b OFFICE SYMBOL (If applicable)	7a NAME OF MONITORING ORGANIZATION Director Defense Nuclear AGency
6c ADDRESS (City, State, and ZIP Code) P.O. Box 548 Aberdeen, MD 21001	7b ADDRESS (City, State, and ZIP Code) Washington, DC 20305-1000
8a NAME OF FUNDING/SPONSORING ORGANIZATION 8b OFFICE SYMBOL (If applicable) SPWE/Gallaway	9 PROCUREMENT INSTRUMENT IDENTIFICATION NUMBER DNA 001-86-C-0249
8c ADDRESS (City, State, and ZIP Code)	10 SOURCE OF FUNDING NUMBERS PROGRAM ELEMENT NO: 62715H; PROJECT NO: RW; TASK NO: RA; WORK UNIT ACCESSION NO: DH018620

11 TITLE (Include Security Classification)
VANE FLOW DIRECTION SENSOR FOR BLAST WAVES

12 PERSONAL AUTHOR(S)
Ethridge, Noel H., and Watson, G. Thomas

13a TYPE OF REPORT	13b TIME COVERED	14 DATE OF REPORT (Year, Month, Day)	15 PAGE COUNT
Technical	FROM 860908 TO 870207	870207	50

16 SUPPLEMENTARY NOTATION
This work was sponsored by the Defense Nuclear Agency under RDT&E RMC Code B3100864662 RW RA 00037 25904D.

17 COSATI CODES		
FIELD	GROUP	SUB-GROUP
19	9	

18 SUBJECT TERMS (Continue on reverse if necessary and identify by block number)
Shock Tube Test, Wind Tunnel Test, Response Time, Precursed Blast Wave, Flow Direction, Precursor, Flow Direction Sensor, Cantilever Beam, Blast Wave

19 ABSTRACT (Continue on reverse if necessary and identify by block number)

The objectives of this study were to review the use of vanes for sensing flow direction and to design a fieldable vane flow direction gage for use in experiments with precursed blast waves, and to recommend a test program for the gage.

Estimates of the requirements for a flow direction sensor were made from the results of an existing numerical calculation of a precursed blast wave. The precursed flow field is very complex, and contains two large vortices and mechanisms for generating smaller scale vortices near the surface. There are high speed flows (Mach 3) present in a jet near the ground, and the response time for a flow direction sensor must be short, 0.2 ms or less if possible.

A rotating wind vane sensor was examined and found to have a response time that was too long. Alternative means of sensing flow direction were investigated and that selected for a gage was measuring the direction of bending of a cantilever beam protruding into the flow by use of strain gages.

20 DISTRIBUTION/AVAILABILITY OF ABSTRACT ☐ UNCLASSIFIED/UNLIMITED ☒ SAME AS RPT ☐ DTIC USERS	21 ABSTRACT SECURITY CLASSIFICATION UNCLASSIFIED
22a NAME OF RESPONSIBLE INDIVIDUAL Bennie F. Maddox	22b TELEPHONE (Include Area Code) (202) 325-7042 22c OFFICE SYMBOL DNA/CSTI

DD Form 1473, JUN 86 *Previous editions are obsolete*

SECURITY CLASSIFICATION OF THIS PAGE
UNCLASSIFIED

18. SUBJECT TERMS (Continued).

Wind Vane
Gage
Vane

19. ABSTRACT (Continued).

The proposed gage has four cylindrical hollow cantilever beams in a cruciform configuration on the end of a supporting shaft. The four output signals describe the flow direction in the vertical plane containing the gage and ground zero, and the horizontal plane. Each cylinder has a natural frequency of about 8300 Hz. Because it is underdamped, the upper usable frequency is about 2080 Hz, with a rise time of 0.12 ms.

The test program recommended includes static calibration, tests of response versus flow angle in a 0.61 meter diameter shock tube at a shock overpressure of about 172 kPa (25 psi), supersonic wind tunnel tests at Mach 1.5, 2.0, and 2.5, and tests in the TRW 0.43 meter shock tube at higher shock pressures with and without dust in flow.

SUMMARY

The objectives of this study were to review the use of vanes for sensing flow direction and to design a fieldable vane flow direction gage for use in experiments with precursed blast waves, and to recommend a test program for the gage.

Estimates of the requirements for a flow direction sensor were made from the results of an existing numerical calculation of a precursed blast wave. The precursed flow field is very complex, and contains two large vortices and mechanisms for generating smaller scale vortices near the surface. There are high speed flows (Mach 3) present in a jet near the ground, and the response time for a flow direction sensor must be short, 0.2 ms or less if possible.

A rotating wind vane sensor was examined and found to have a response time that was too long. Alternative means of sensing flow direction were investigated and that selected for a gage was measuring the direction of bending of a cantilever beam protruding into the flow by use of strain gages.

The proposed gage has four cylindrical hollow cantilever beams in a cruciform configuration on the end of a supporting shaft. The four output signals describe the flow direction in the vertical plane containing the gage and ground zero, and the horizontal plane. Each cylinder has a natural frequency of about 8300 Hz. Because it is underdamped, the upper usable frequency is about 2080 Hz, with a rise time of 0.12 ms.

The test program recommended includes static calibration, tests of response versus flow angle in a 0.61 metre diameter shock tube at a shock overpressure of about 172 kPa (25 psi), supersonic wind tunnel tests at Mach 1.5, 2.0, and 2.5, and tests in the TRW 0.43 metre shock tube at higher shock pressures with and without dust in the flow.

PREFACE

This project was sponsored by the Defense Nuclear Agency (DNA) under Contract No. DNA001-86-C-0249, with Dr. Charles Gallaway (SPAS) of the Shock Physics Directorate as the Contract Technical Manager. Mr. John H. Keefer, Director of the Aberdeen Research Center, provided guidance and technical advice to the project.

The authors express appreciation to Mr. Willis Jackson and others of the Aberdeen Research Center that contributed to the work, and to Dr. Allen Kuhl, R&D Associates, Marina del Rey, California, for computer plots of a precursed blast wave.

CONVERSION TABLE FOR U.S. CUSTOMARY TO METRIC (SI) UNITS OF MEASUREMENT

and Other Conversion Factors

Conversion Factors With an Asterisk (*) are Exact

to convert from	to	multiply by
angstrom	meters (m)	1.000 000*E-10
atmosphere (normal)	kilopascal (kPa)	1.013 250*E+02
bar	kilopascal (kPa)	1.000 000*E+02
barn	meter^2 (m^2)	1.000 000*E-28
calorie (thermochemical)	joule (J)	4.184 000*E+00
cal (thermochemical)/cm^2	megajoule/m^2 (MJ/m^2)	4.184 000*E-02
degree (angle)	radian (rad)	1.745 329 E-02
degrees Fahrenheit (temperature)	kelvin (K)	$T_K = (t°_F + 459.67)/1.8$
electron volt	joule (J)	1.602 190 E-19
erg	joule (J)	1.000 000*E-07
erg/second	watt (W)	1.000 000*E-07
foot	meter (m)	3.048 000*E-01
foot-pound-force	joule (J)	1.355 818 E+00
inch	meter (m)	2.540 000*E-02
kilotons (KT)	terajoule (TJ)	4.184 E+00
ktap	newton-second/m^2 (N-s/m^2)	1.000 000*E+02
micron	meter (m)	1.000 000*E-06
micron Hg, 0°C (pressure)	pascal (Pa)	1.333 22 E-01
mil	meter (m)	2.540 000*E-05
mile (international)	meter (m)	1.609 344*E+03
ounce	gram (g)	2.843 952 E+01
pound-force (lb avoirdupois)	newton (N)	4.448 222 E+00
pound-force inch	newton-meter (N·m)	1.129 848 E-01
pound-force/inch	newton/meter (N/m)	1.751 268 E+02
pound-force/foot^2	kilopascal (kPa)	4.788 026 E-02
pound-force/inch^2 (psi)	kilopascal (kPa)	6.894 757 E+00
pound-mass (lbm avoirdupois)	kilogram (kg)	4.535 924 E-01
pound-mass-foot^2 (moment of inertia)	kilogram-meter^2 (kg·m^2)	4.214 011 E-02
pound-mass/foot^3 (density)	kilogram/meter^3 (kg/m^3)	1.601 846 E+01
rad (radiation dose absorbed)	gray (Gy)	1.000 000*E-02
shake	second (s)	1.000 000*E-08
torr (mm Hg, 0°C)	pascal (Pa)	1.333 22 E+02

TABLE OF CONTENTS

LIST OF ILLUSTRATIONS

SECTION 1

INTRODUCTION

The blast wave from a nuclear explosion is affected by the hot layer of gas produced on the ground surface by the thermal radiation from the fireball. This hot layer with its higher sound speed alters the propagation of the blast wave so that a wave called the precursor extends into the hot layer in advance of the main shock wave. The presence of the hot layer causes the development of a very complex flow field with large and fast changes in flow variables with time and position. For targets on the ground, the blast loading can be radically altered. The development of an understanding of precursed blast waves and a capability to predict the flow fields is essential for loading predictions on targets.

Experimental and computational studies of precursed flow show that large changes occur in the direction of flow. At this time there is no suitable sensor for measuring flow direction in the precursed blast wave experiments. Experiments have been conducted and more are planned that utilize a helium layer at the ground surface to simulate the high sound velocity hot layer. Flow direction sensors are needed to measure flow direction versus time in and above the helium layer. The data obtained will be used with data from other types of sensors for diagnosis of the blast flow field and for comparison with code predictions.

The tasks to be performed in this study were as follows:

1. Conduct a literature survey to review the use of vanes for sensing flow direction. Determine the characteristics of the precursor environment to understand its severity. Establish the minimum requirements for a vane flow direction sensor.

2. Design a fieldable flow direction sensor which is ready for construction and evaluation, and estimate its cost. Recommend a program to test and certify the sensor.

SECTION 2

PRECURSOR ENVIRONMENT

Precursors that occurred on nuclear explosions produced enhanced loading on ground targets and increased the radii for damage to some types of military equipment by as much as 50 percent. The precursor flow fields contained dust, with the amount of dust varying with test location, ground surface, and yield. The dust added to the loading on targets, and caused damage directly by sandblasting surfaces and plugging gage openings. Dynamic pressures were increased by factors ranging from two to four above those that would occur for undisturbed blast waves. Dynamic pressure waveforms were characterized by a distorted shape and large and rapid oscillations. The environment was severe for both targets and gages.

Recent work has shown that the primary factor affecting precursor production and its characteristics is the high sound speed layer produced by the thermal radiation from the explosion. Experiments using a helium layer to produce the high sound speed layer on a surface have been conducted in shock tubes and on high explosive tests where charges have been on the surface and suspended above the surface. Precursors were produced with shock wave configurations and pressure waveforms similar to those observed on nuclear tests.

Reference 1 describes the fluid dynamics of precursors and the requirements for simulating them using a helium layer. The results of an inviscid 2-D numerical calculation of a clean air (no dust) blast flow field with a helium layer modeling the high sound speed layer are presented to display the characteristics of the precursor flow field. The results are presented in terms of a 1-KT nuclear explosion at a height-of-burst of 61 m (200 ft) and a helium layer 0.061 m (0.2 ft) thick.

Figure 1a depicts the isopycnics, Figure 1b the isobars, Figure 2a the velocities fixed at the moving stagnation point, and Figure 2b the velocities in laboratory coordinates in the precursor region at a time of 0.160 $s/KT^{1/3}$.

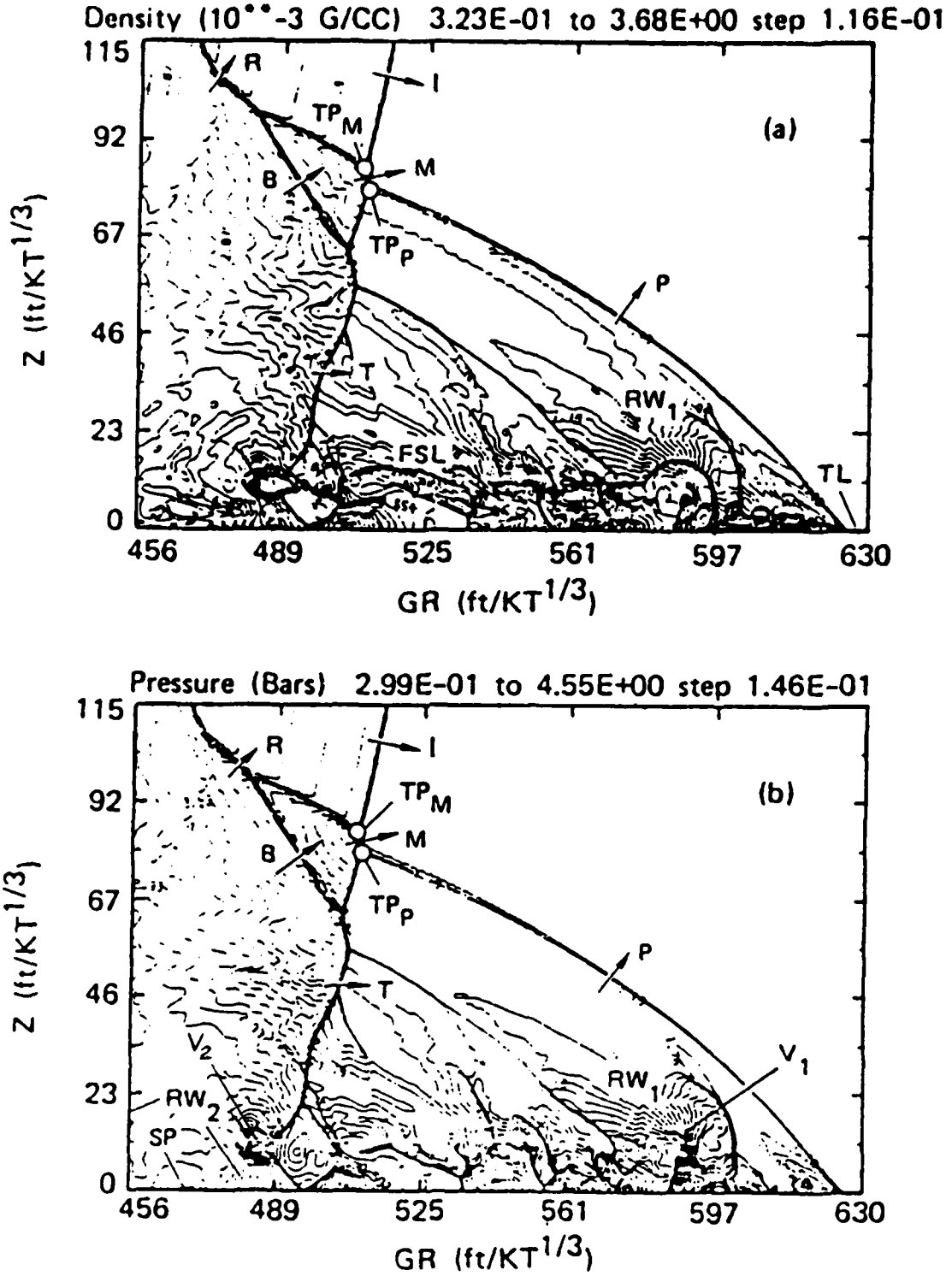

Figure 1. Density and pressure contours for a numerical calculation of a precursed blast wave.

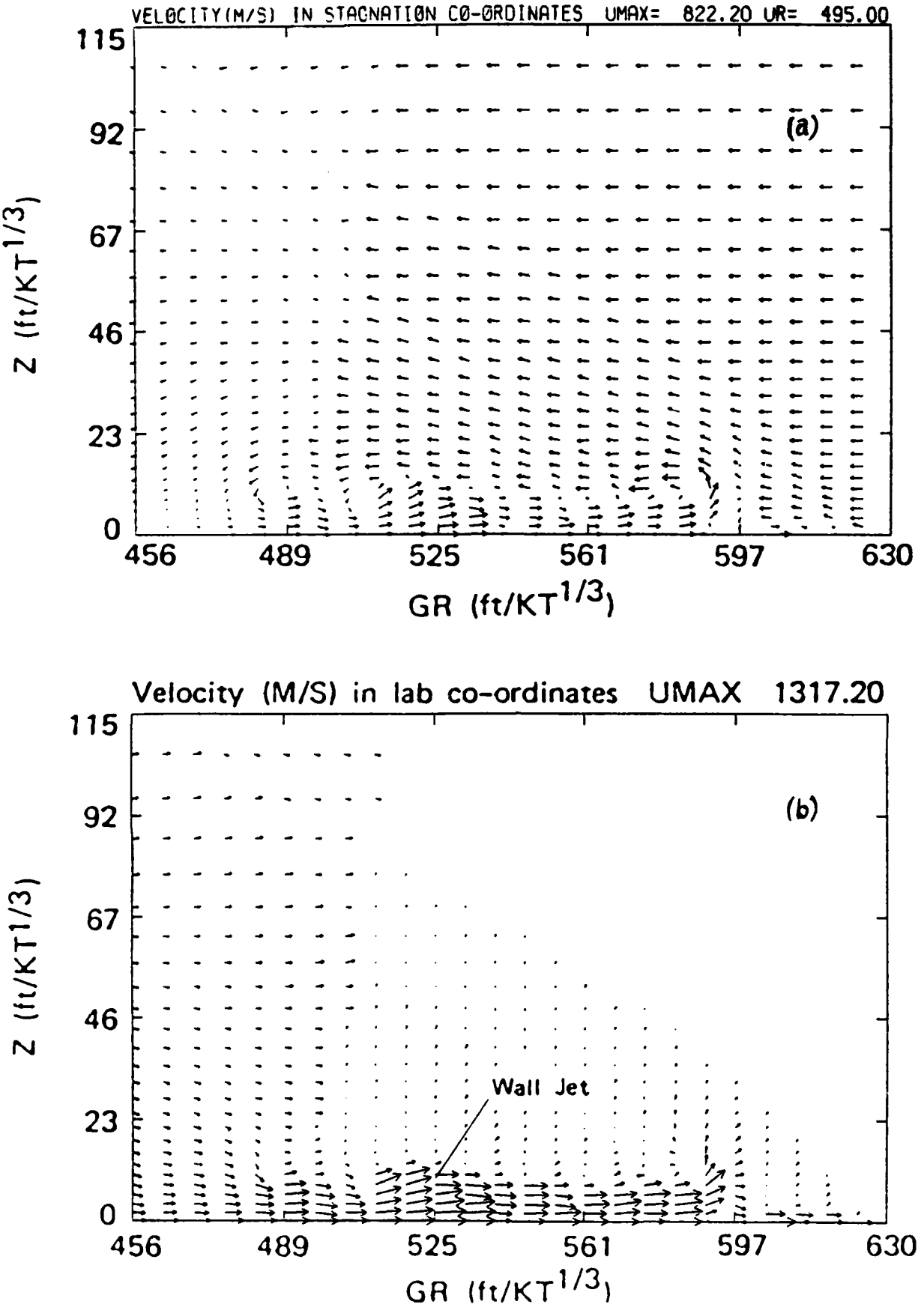

Figure 2. Velocity vectors from a numerical calculation of a precursed blast wave in precursor-fixed coordinates and laboratory coordinates.

These figures were taken from Reference 1, except for Figure 2a (Ref. 2). The incident shock has run forward of the main shock in the high sound speed layer (TL) at the surface, forming the oblique precursor shock (P). The precursor shock P causes the gases in the high sound speed layer to rise upward, which in turn induces air to move in underneath the lofted gas. This action forms a high velocity (Mach 3) wall jet, which is very obvious in Figures 2a and 2b.

The explanation of the figures from Reference 1 follows, since that reference may not be readily available.

> "In precursor-fixed coordinates (see Figure 2A), air from above the thermal layer flows through the oblique precursor shock P and is thus deflected upward, is turned approximately parallel to the ground by rarefaction wave RW_1, and is turned toward the ground by the turning shock T. This flow then partially stagnates at the 'moving stagnation point' SP, and is accelerated forward by rarefaction wave RW_2 which supports the wall jet flow. In effect, rarefaction waves RW_1 and RW_2 correspond to the pressure fields associated with two large-scale vortex structures, V_1 and V_2, with positive vorticity. They induce counter-clockwise rotational velocities which add to the background motion. Hence, velocities in laboratory coordinates are increased underneath each vortex and decreased above each vortex. Velocities on the wall tend to peak and pressures drop under each vortex. The above features correspond to the laminar evolution of the wall jet.
>
> "Actually, the wall jet evolves chaotically. It consists of a free shear layer (FSL) on top of the jet and a wall boundary layer which was not modeled here. The free shear layer is hydro-dynamically unstable in the Kelvin-Helmholtz sense. Small perturbations amplify by an <u>inviscid</u> mechanism,* and agglomerate in coherent vortex structures -- this code's representation of the turbulent mixing in the free layer region. The wall jet acts like a supersonic channel flow. Area variations induced by the coherent structures on FSL create 'barrel shocks' and rarefaction

---

* grad ρ x grad p

waves embedded in the wall jet. Corrugations on top of the free shear layer induce additional oblique shocks in the flow above the jet.

"These shocks induce an additional nonlinear wrenching of the free shear layer. In the latter stages, the mixing in the free shear layer extends all the way to the ground. This spreads the jet momentum vertically, and eventually leads to the turbulent self-destruction of the wall jet in the precursor cleanup phase."

The discussion above indicates that there are at least two large scale vortices V_1 and V_2 to be expected in the precursor flow field and smaller scale vortices generated by the wall jet interaction with the free shear layer above it and the boundary layer below it. Large changes in flow direction may occur for a sensor placed so that a vortex passes over it.

The flow field in Figure 2b displays a variety of flow direction changes. Along the precursor shock P the vertical angles of flow vary from about 40 degrees near ground level to about 60 degrees near the main shock. The velocity magnitudes are relatively small compared to the wall jet velocities.

At 182 m (597 ft) at a height of about 3.7 m (12 ft) in the vortex V_1 the velocity changes direction from an angle of about 15 degrees with respect to the horizontal to 90 degrees at 180 m (590 ft) to 180 degrees at 178 m (583 ft), a change of 165 degrees in 4.27 m (14 ft). Assuming a velocity relative to the ground of 800 m/s (Figure 2a), the change in angle of 165 degrees will occur in about 0.0053 s as the flow field sweeps past a sensor located at 180 m (590 ft), corresponding to a rate of 3.1×10^4 degrees per second.

Lower in elevation under the forward edge of the vortex V_1 at 182 m (597 ft) at a height of about 1.5 m (5 ft) the velocity angle change is about 40 degrees over a distance of 2.2 m and a time of 0.0027 s.

Between 153 m (503 ft) and 155 m (510 ft) near the upper part of the wall jet at a height of about 1.8 m (6 ft) the velocity changes direction about 30

degrees over a distance of 2.2 m. Assuming the velocity relative to the ground is 800 m/s, the time for the change is 0.0027 s.

In the wall jet near the surface the angular changes in direction shown in Figure 2b are about 10 degrees or less. However, the numerical model does not include a boundary layer model and is limited in resolution, so that larger angular variations may appear in a more detailed modeling.

The maximum rate of change noted above was for a change of 90 degrees in 0.00275 s for the large scale vortex V_1. At 0.040 KT or 20 tons of HE, the time interval would be 0.00094 s, and for 0.001 KT or 1000 lbs of HE, 0.000275 s. To measure a change of 90 degrees in 0.00275 s in a 1-KT yield with a resolution of 5 degrees would require a sensor response time of 0.15 ms.

Considering the angular rates calculated above and the expectations of additional vorticity in an experiment, the response time for a vane flow direction sensor should be about 0.2 ms or less, "as fast as possible."

The numbers above were obtained by reading from the figures. Improved estimates could be obtained by processing the hydrocode data to read out velocity direction and magnitude versus elevation at several ground ranges.

SECTION 3

ROTATION WIND VANE RESPONSE CHARACTERISTICS

Simple wind vanes have been in use for many years to indicate wind direction. Such vanes consist of an aerodynamic surface attached to an arm that is free to rotate on a pivot, and a mass at the end of the arm away from the vane that statically balances the vane. A properly designed vane will align itself parallel to the air flow, and if displaced, will return to its former equilibrium position through a few oscillations of rapidly diminishing amplitudes. The design of such wind vanes has progressed. Vanes have been used in a variety of meteorological and aircraft applications for a wide range of flow conditions.

A small wind vane that rotates to align itself parallel to the air flow was examined as a candidate for a flow direction sensor. The response of such a vane for small deflections will be used to judge its promise for blast measurements.

For small deflections the equation describing the vane response is analogous to that for a spring-mass system with viscous damping undergoing linear free oscillations. The derivation of the equation is given in both References 3 and 4, and is summarized below.

Figure 3 shows the schematic of a simple vane. The wind vector $\bar{U}$ makes an instantaneous angle β with respect to the vane. The vane experiences an aerodynamic force F acting normal to its surface at its center of pressure, a distance r from the axis of rotation. The vane velocity at the center of pressure is $rd\beta/dt$. In coordinates moving with the vane, the air velocity relative to the vane is $\bar{U}_V$, and the instantaneous angle of attack β_V is, for small β,

$$\beta_V \cong \beta + \frac{r}{U}\frac{d\beta}{dt} \qquad (1)$$

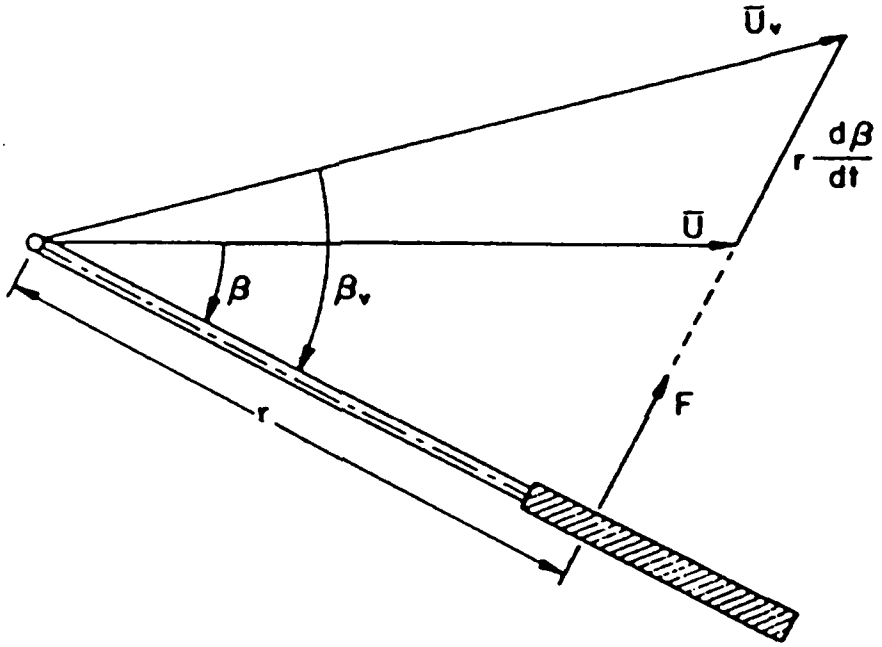

Figure 3. Schematic plan view of a vane.

When the vane is displaced from its center of equilibrium, the normal force F produces a returning torque Fr. For small β, $U_v = |\bar{U}_v| = U$. Then the aerodynamic force F normal to the vane is

$$F = (\rho U^2/2)A\ C_L \cos \beta_v, \tag{2}$$

where C_L is a lift coefficient, A is the projected vane area in the plane of zero angle of attack, and ρ is the density of the air.

For small β_v,

$$C_L \cong \frac{\partial C_L}{\partial \beta} \Big|_o \beta_v, \quad \cos \beta_v \cong 1 \tag{3}$$

Let $a = \frac{\partial C_L}{\partial \beta} \Big|_o$. Then $F = (\rho U^2/2)A\ a\ \beta_v$ (4)

Under dynamic equilibrium,

$$I \frac{d^2\beta}{dt^2} = -F\ r \tag{5}$$

where I is the moment of inertia of the oscillating vane about the rotation axis.

A unit angle torque is defined as

$$N = Fr/\beta_v = (\rho U^2/2)\ A\ r\ a \tag{6}$$

and upon its substitution in equation (5) yields

$$I \frac{d^2\beta}{dt^2} = -N\beta_v = -N(\beta + \frac{r}{U} \frac{d\beta}{dt})$$

$$I \frac{d^2\beta}{dt^2} + \frac{Nr}{U} \frac{d\beta}{dt} + N\beta = 0 \tag{7}$$

The aerodynamic damping constant D is given by

$$D = Nr/U \tag{8}$$

Thus the equation of vane motion can be written as follows:

$$\frac{d^2\beta}{dt^2} + \frac{D}{I}\frac{d\beta}{dt} + \frac{N}{I}\beta = 0 \tag{9}$$

In terms of the angular natural frequency ω_n and the damping ratio ζ, the equation is

$$\frac{d^2\beta}{dt^2} + 2\zeta\omega_n \frac{d\beta}{dt} + \omega_n{}^2\beta = 0 \tag{10}$$

where

$$\omega_n = (N/I)^{\frac{1}{2}} = ([\rho U^2/2]\ Ara/I)^{\frac{1}{2}} \tag{11}$$

$$\zeta = \frac{D}{2(IN)^{\frac{1}{2}}} = (\rho r^3 Aa/8I)^{\frac{1}{2}} \tag{12}$$

The natural frequency ω_n varies linearly with wind speed U, while ζ is a property of the vane alone, providing that the speed range is small enough that the lift characteristics do not change.

The time lapse for oscillations to decrease from a peak amplitude of β_o at t = 0 to some specified peak amplitude β_R at t_R is defined as the vane response time (Ref. 4). This vane response time can be obtained from the expression for the amplitude of the envelope of the oscillations,

$$\beta = \beta_o \exp(-\zeta\omega_n t) \tag{13}$$

at $t = t_R$, $\ell n\ (\beta_o/\beta_R) = \zeta\omega_n t_R$, and

$$t_R = \frac{\ell n\ (\beta_o/\beta_R)}{\zeta\omega_n} \tag{14}$$

Upon substituting the relations in equations (11) and (12) for ω_n and ζ, the result obtained is

$$t_R = \frac{4I\ \ln(\beta_o/\beta_R)}{\rho Ar^2 aU} = \frac{(2I)^{\frac{1}{2}}\ \ln\ (\beta_o/\beta_R)}{(\rho Ara)^{\frac{1}{2}}\ \zeta U} \tag{15}$$

The vane response time increases with increasing moment of inertia I, and decreases with air velocity U. Fortunately for blast wave applications the changes in flow direction are expected to occur in the early portion of the blast wave where the air velocities are near maximum.

SECTION 4

TIME RESPONSE FOR A CANDIDATE VANE DESIGN

A vane for use in precursed blast waves will be subjected to supersonic, transonic, and subsonic flows. The stability of a vane over such a span of flow regimes is of particular concern. The candidate vane design selected was derived from Reference 5, which describes tests of different vane configurations for a range of Mach numbers from 0.3 to 3.0 and for angles of attack ranging from -3 to +24 degrees. The report describes a vane that was dynamically stable over the entire Mach number range. Figure 4 shows the details of the vane configuration and the supporting boom. Two sets of vanes are shown, one to measure angle of attack and the other, sideslip. The vane configuration shown is the only one found in the literature search that was tested over such a range of Mach numbers and angles of attack.

For application to blast wave measurements, the configuration shown in Figure 4 was scaled down by a factor of about seven to the smallest boom that seemed practical for use in the field. Figure 5 shows the configuration selected. The vanes are to be made of magnesium alloy, selected for low mass and high stiffness, the shaft of hardened steel, and the counter-weight of tungsten to minimize size.

Parameters for calculating the time response and natural frequency are as follows:

$I = 5.75 \times 10^{-8}$ kgm^2
$A = 1.06 \times 10^{-4}$ m^2
$r = 1.1 \times 10^{-2}$ m
$a = 1.6$

The parameter a was calculated using the relation

$$a = 2\pi \frac{AR}{2 + AR} \tag{16}$$

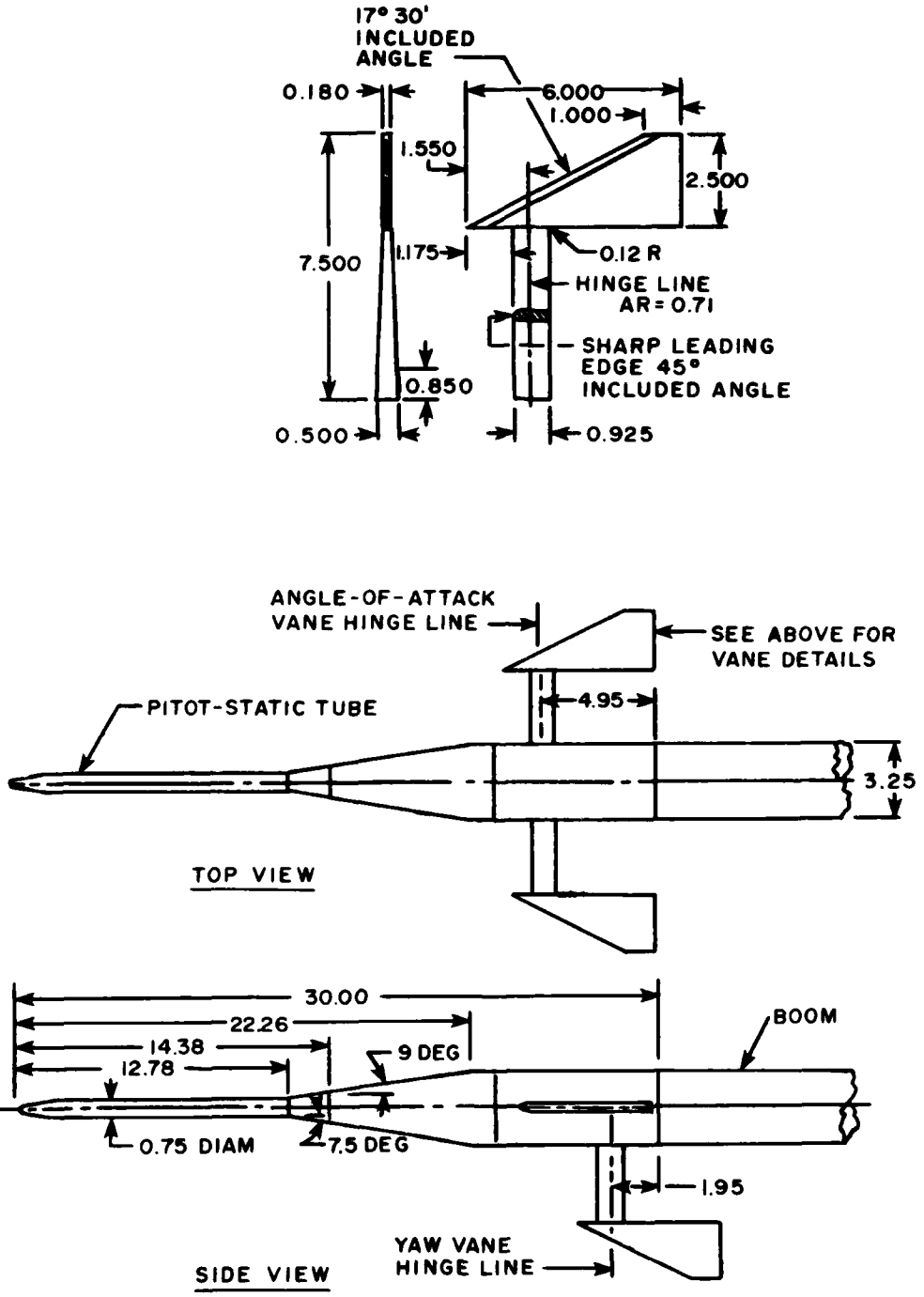

ALL DIMENSIONS IN INCHES

Figure 4. Schematic of flight path accelerometer with movable vanes from Reference 5.

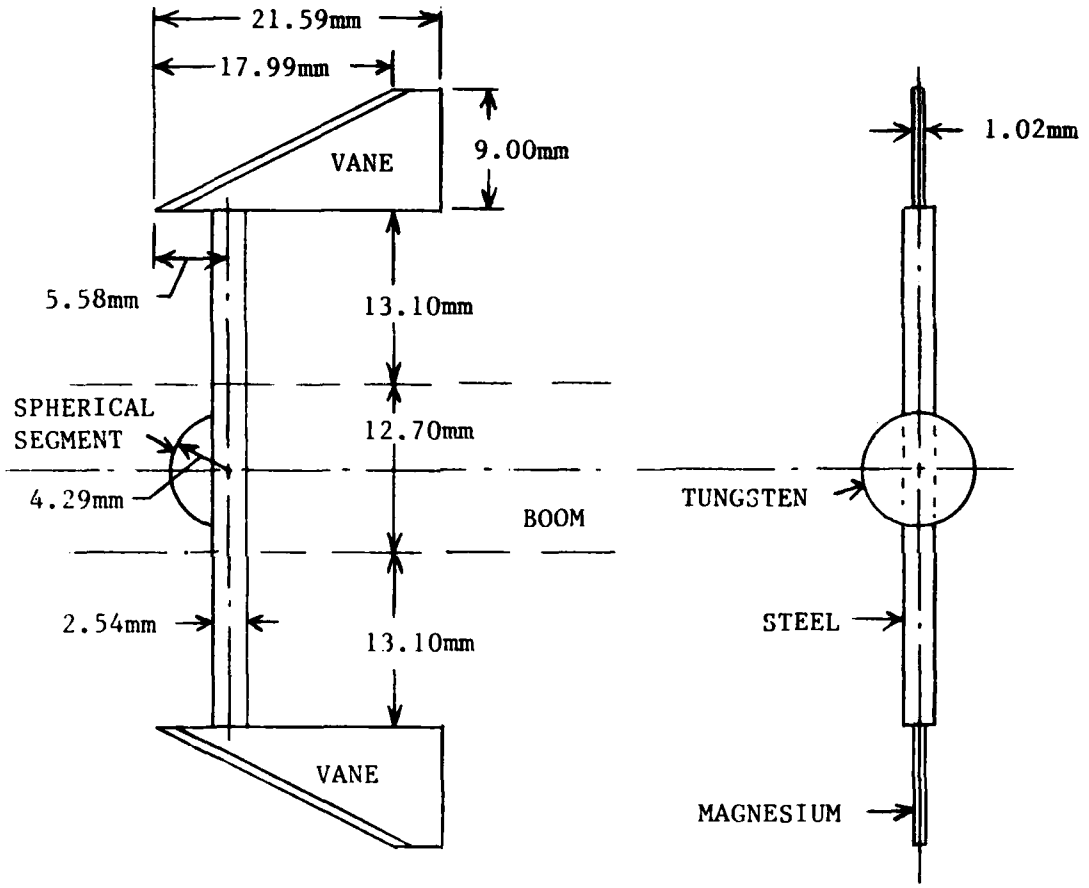

Figure 5. Rotating component of candidate vane sensor.

where A_R is the aspect ratio, which is 0.71 for the particular vane configuration. This relation was found to be in fair agreement with experiments at low velocities in Reference 4.

Calculation of the vane response characteristics were made for shock waves of 103 kPa (15 psi), 207 kPa (30 psi), and 345 kPa (50 psi) at an ambient pressure of 86.2 kpa (12.5 psi), an ambient density of 1.074 kg/m^3, and a sound velocity of 335 m/s (1100 ft/s). The calculations were made for conditions immediately behind the shock front, so that density and flow velocities were obtained from shock front relations given in Reference 6. The results are given in Table 1.

The value of t_R listed is that time for the amplitude of the oscillation to decrease by one-half, i.e., $\ln \beta_o/\beta_R = 0.693$. The response times are long compared to the usual response times sought for blast wave measurements, and are longer still for a further decrease in oscillation amplitude.

The experimental data in Reference 4 show that the damping for low speeds may be about twice as large as that predicted by equation (12) for a delta-shaped vane. However, even with response times reduced by a factor of two, they are longer than desired. A factor that will complicate interpretation of a record from such a vane in flow changing rapidly in flow direction is that the response time depends on the velocity of the flow.

Another measure of vane performance is the "direction constant," defined in Reference 7 as the length of air passage moving at speed U before the vane can attain one cycle in its direction response. It is given by the relation

$$T_n U = 2\pi \left(\frac{2I}{\rho A r a}\right)^{1/2} \tag{17}$$

where

$$T_n = 1/f_n = 2\pi/\omega_n \tag{18}$$

Values for f_n, T_n, and T_nU are given in Table 1. The values of T_nU are approximately one metre, but they are not constant. Because of the low damping the vane will require several cycles to settle, so the length of air passage at speed U before the vane is near equilibrium will be about three metres or more.

Because of the slow response time and low spacial resolution the movable vane sensor of the type shown in Figure 5 does not seem to be suitable for use in blast waves.

Table 1. Vane response characteristics at shock front conditions.

Shock Overpressure (kPa)	Shock Overpressure (psi)	ρ (kg/m^3)	U (m/s)	ω_n (/s)	f_n (/s)	T_n (s)	ζ	$t_{R½}$ (s)	T_nU (m)
103	15	1.86	202	1110	176	0.0057	0.030	0.0210	1.14
207	30	2.44	329	2070	330	0.0030	0.035	0.0097	1.00
345	50	3.03	455	3190	507	0.0020	0.039	0.0056	0.90

SECTION 5

ALTERNATIVE FLOW DIRECTION SENSORS

A technique for determining flow direction and magnitude is that of placing a body of simple shape in the flow and measuring the components of force acting upon it. Reference 8 describes a small rectangular cantilever beam anemometer. It is fragile and presents a changing area to the flow as flow angle varies, and therefore is unsuitable for the present application. Spheres have been used for air and water flow measurements (Ref. 9). Spheres were used on past nuclear tests and on HE tests with limited success. A cantilever beam gage with a sensitive center section was used on HE tests (Refs. 10 and 11). The response times of these gages are too long for the application of interest.

A cylindrical cantilever beam mounted on a single component balance is described in Reference 12. Reference 13 describes a hollow cylindrical cantilever beam designed for use in a blast wave. Two versions were built with natural frequencies of 500 and 1000 Hz and tested in a shock tube, where the performance was judged to be satisfactory.

One gage was 0.0572 m (2.35 in.) in diameter and 0.328 m (12.9 in.) long, and the other was the same diameter but 0.231 m (9.10 in.) long. They were instrumented for longitudinal strain with strain gages spaced at intervals of 90 degrees around the base of each beam. These gages were large and slow, but the concept seems most appropriate of those found in the literature for the current application. Therefore a small hollow cylindrical cantilever beam will be considered as a means of indicating flow direction.

SECTION 6

CANTILEVER BEAM FLOW DIRECTION SENSOR

The proposed configuration for using the hollow cylindrical beam as a flow direction sensor is shown in Figures 6 and 7. The configuration shown on the left in Figure 6 measures flow direction in the horizontal plane and in the vertical plane passing through the gage and ground zero. The output of the beams on the same axis are added, providing higher signal levels and some compensation for the lack of symmetry and partial shielding effects for off angle flow. Figure 7 shows a cross-section of this configuration.

To measure flow direction in the vertical plane perpendicular to the radius from ground zero will require a beam mounted separately, as shown to the right in Figure 6. The end loading on the beam will be significant, and higher sensitivity to bending will be required. A beam with only a sensitive center section (Refs. 10 and 11) may be required for this orientation.

Strain gages were selected as the means of measuring beam deflection because they represent a well known technology and can be connected easily so that the output of the two beams on the same axis are added together. The strain gages are mounted to measure longitudinal strain at 90 degree intervals around the inside surface of the beam at its base.

The beams are made as small as can be instrumented using strain gages. This corresponds to a diameter of about 0.010 m (0.4 in.) if the strain gages are mounted on the outside of the cylinder, and 0.0127 m (0.5 in.) if the strain gages are mounted inside the cylinder. The two factors affecting size are the requirement for adequate access to install the gages and a minimum curvature of the surface on which the gages are to be mounted (Ref. 14).

The output from each beam will be two signals indicating the magnitude of bending and hence force in two perpendicular directions, so that force direction and magnitude in the plane perpendicular to the axis can be determined. Because of the varying drag coefficient across the subsonic,

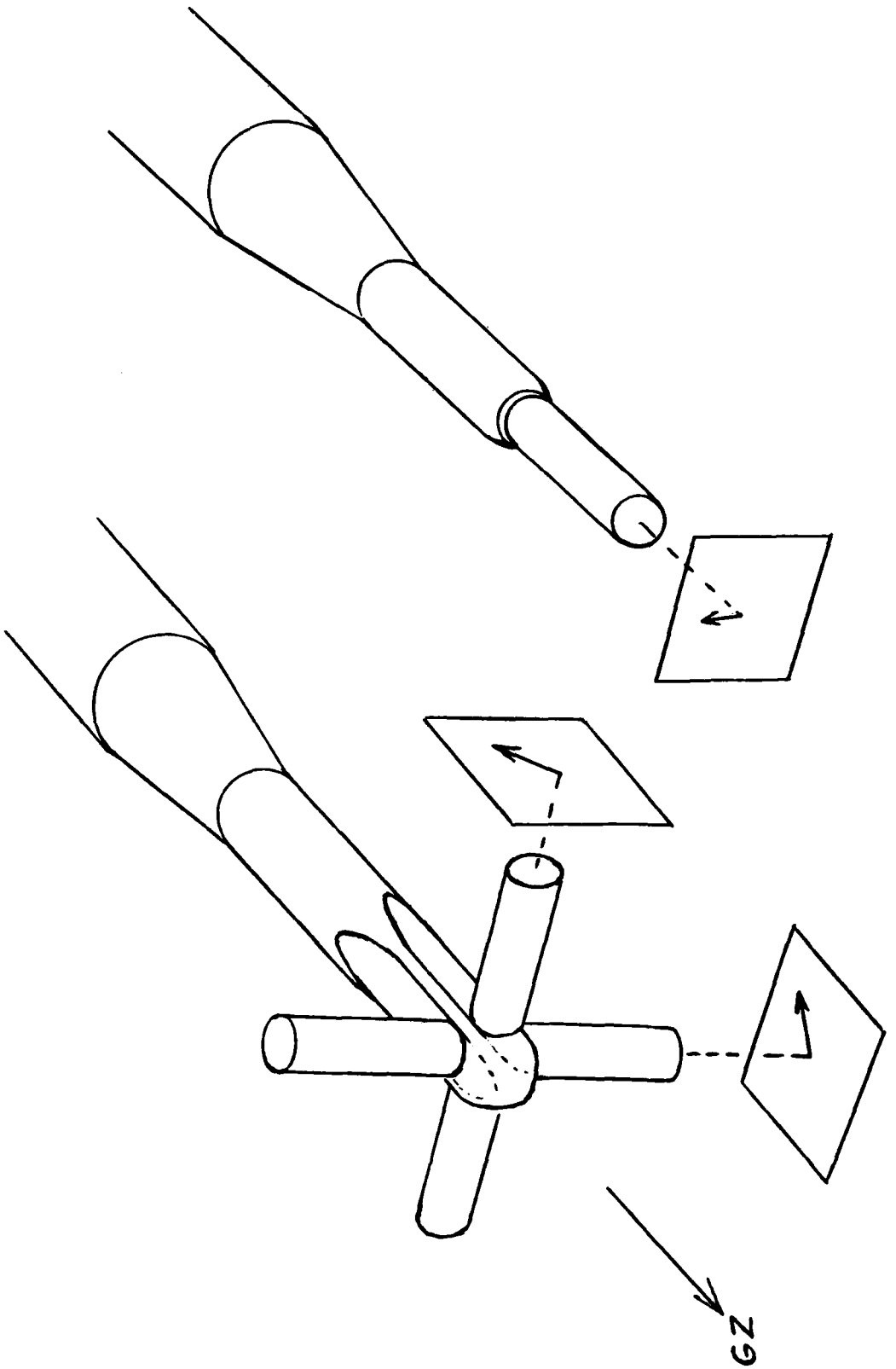

Figure 6. Cantilever beam flow direction sensor.

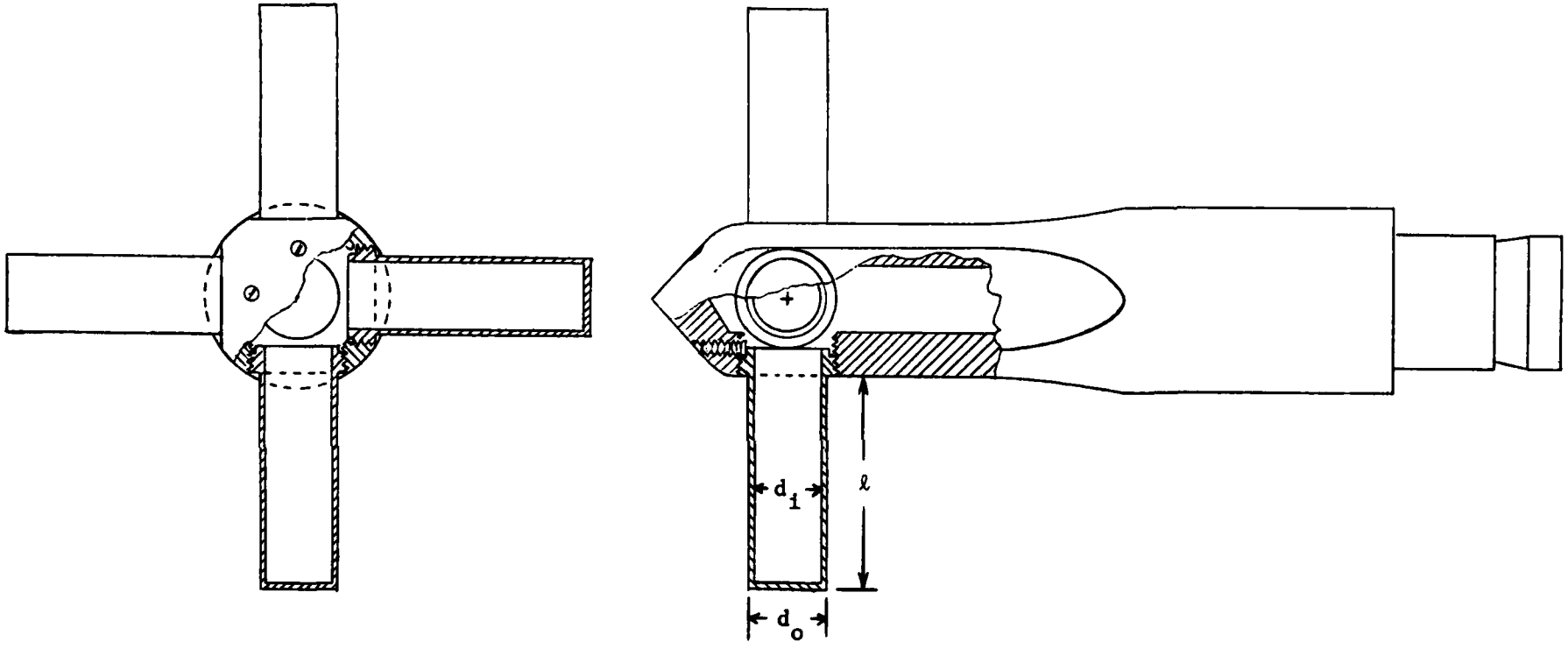

Figure 7. Cross-section of two-axis cantilever beam flow direction sensor.

transonic, and supersonic flow regimes and presence of dust in the flow, the force component measured cannot be used to make a quantitative determination of dynamic pressure.

To obtain estimates of the strain at the base of the beam, simple beam bending relations are used (Ref. 15).

Strain in a fiber in a bent beam is

$$\varepsilon = h/R \tag{19}$$

where h = distance from neutral axis, center of beam,
R = radius of curvature of the beam.

Now

$$1/R = \left(\frac{d^2y}{dx^2}\right) \Big/ \left(1 + \left(\frac{dy}{dx}\right)^2\right)^{3/2} \tag{20}$$

where $y = f(x)$, the function describing the deflection y of the beam versus x distance along its length.

The slope dy/dx is very small, so that its square in equation (20) can be neglected, so that

$$1/R \cong \frac{d^2y}{dx^2} \tag{21}$$

and

$$\varepsilon = h \frac{d^2y}{dx^2} \tag{22}$$

For a uniformly distributed load on a cantilever beam (Ref. 15),

$$y = \frac{w}{24EI} x^2 (x^2 - 4\ell x + 6\ell^2) \tag{23}$$

where w = force per unit length

ℓ = length of beam

x = distance from supported end.

$$\frac{d^2y}{dx^2} = \frac{w}{24EI} \quad (12x^2 - 24\ell x + 12\ell^2) \tag{24}$$

Then

$$\varepsilon = h \cdot \frac{w}{24EI} \quad (12x^2 - 24\ell x + 12\ell^2) \tag{25}$$

For $x = 0$, the strain at the base is

$$\varepsilon = \frac{wh}{2EI} \cdot \ell^2 \tag{26}$$

In a blast wave flow, $w = C_D A \cdot Q/\ell$

where C_D = drag coefficient

A = area = $\ell \cdot d_o$

d_o = outside diameter of beam

Q = dynamic pressure = $\rho U^2/2$

For strain gages on the inside of the beam, $h = d_i/2$, where d_i is the interior diameter of the beam.

Substituting these values in equation (26) produces the following relation for the maximum strain on the inside wall:

$$\varepsilon = C_D \, Q \, \frac{d_o \, d_i \, \ell^2}{4 \, EI} \tag{27}$$

The natural frequency of vibration of a cantilever beam of uniform section is given by (Ref. 16)

$$f_n = (3.52 / 2\pi) (EI/m\ell^4)^{\frac{1}{2}} \tag{28}$$

where m = mass per unit length.

For the hollow cylindrical beam of interest here

$$I = (\pi/64) (d_o^4 - d_i^4) \tag{29}$$

Let $D_o = d_o/\ell$ and $D_i = d_i/\ell$.

Then equation (28) can be written as follows:

$$f_n = \frac{3.52}{8\pi\ell} \quad \frac{E}{\rho_m} \left[\frac{(D_o^4 - D_i^4)}{(D_o^2 - D_i^2)} \right]^{\frac{1}{2}} \tag{30}$$

where ρ_m = density of beam material.

The proposed material for the beams is 17-4PH stainless steel, condition H900 (Ref. 14). Using $E = 200 \times 10^6$ kPa (29×10^6 psi) and $\rho_m = 7.835 \times 10^3$ kg/m^3 (0.283 lb/in.^{3}), equation (30) becomes as follows:

$$f_n = \frac{707.5}{\ell} \left[\frac{D_o^4 - D_i^4}{D_o^2 - D_i^2} \right]^{\frac{1}{2}} \tag{31}$$

where ℓ is in meters, and

$$f_n = \frac{27860}{\ell} \left[\frac{D_o^4 - D_i^4}{D_o^2 - D_i^2} \right]^{\frac{1}{2}} \qquad (32)$$

where ℓ is in inches.

The beam will be highly underdamped, so that the usable upper frequency will be about 0.25 f_n.

The output signal from the gage should be filtered prior to recording. The gage system should be set up so that the oscillations remain linear, and the electrical output remains linear and it is not clipped prior to filtering.

The proposed cantilever beam has the following dimensions:

ℓ = 0.0406 m (1.60 in.)
d_o = 0.0147 m (0.58 in.)
d_i = 0.0127 m (0.50 in.)

The maximum strain on the inside wall from equation (27) is .000257. For a value of Q of 689 kPa (100 psi), C_D = 1.0, E = 200 x 10^6 kPa (29 x 10^6 psi), and the dimensions listed above, equation (27) produces a strain of .000257.

For semiconductor strain gages with a gage factor of 150 in a two-arm bridge to measure bending, the output from a beam will be 19.3 mv/v. At 5 volts excitation the output will be 96.5 millivolts, which is adequate.

The natural frequency of the beam, calculated from equation (31), is 8330 Hz. Because of the low damping the upper usable frequency will be about 0.25 f_n = 2080 Hz, with a period of 0.00048 s and a rise time at about 0.00012 s. This time is short enough to provide a useful sensor according to the discussion in Section 2 of this report.

The cost estimates for prototype gages are as follows:

	2-Beam	4-Beam
Hardware:		
Beams	$ 280	$ 560
Beam Probe	$ 530	$ 540
	$ 810	$1100
Strain Gaging [$500/beam]	$1000	$2000
Static Calibration	$ 300	$ 600
TOTAL	$2110	$3700

These costs apply for gage designs that have been evaluated and found to be satisfactory. No development costs are included.

The 2-Beam version will measure flow direction in the vertical plane in the line through the gage and ground zero. The 4-Beam version will measure flow direction in the horizontal plane and in the same vertical plane as the 2-Beam version.

SECTION 7

RECOMMENDED TEST PROGRAM

Evaluation and certification of the flow direction sensor will require static testing, and tests in shock tubes and wind tunnels. In static tests its output versus direction of force applied will be measured and its angular resolution, symmetry of response, linearity and hysteresis determined. After the static tests have been completed a series of dynamic tests in both shock tubes and wind tunnels will be conducted.

7.1 STATIC CALIBRATION.

For the static calibration a concentrated transverse load P will be imposed on the end of the cantilever beam, as shown in Figure 8. The angle Θ is the angle between the line of action of the load P and the strain gage location. For a selected angle Θ, the outputs from the strain gage bridges will be recorded as the load is increased in steps from zero to maximum and decreased in steps to zero. This procedure will be followed for different values of Θ. The data obtained will be examined to evaluate the linearity and symmetry of strain response versus angle of loading.

The data will also be compared with a relation derived using equation (22). For the cantilever beam with a concentrated transverse load P at its free end, the deflection is (Ref. 15)

$$y = \frac{Px^2}{6EI} \quad (3\ell - x^3), \tag{33}$$

and

$$\frac{d^2y}{dx^2} = \frac{P}{EI} \quad (\ell - x). \tag{34}$$

From equation (22) the bending strain is

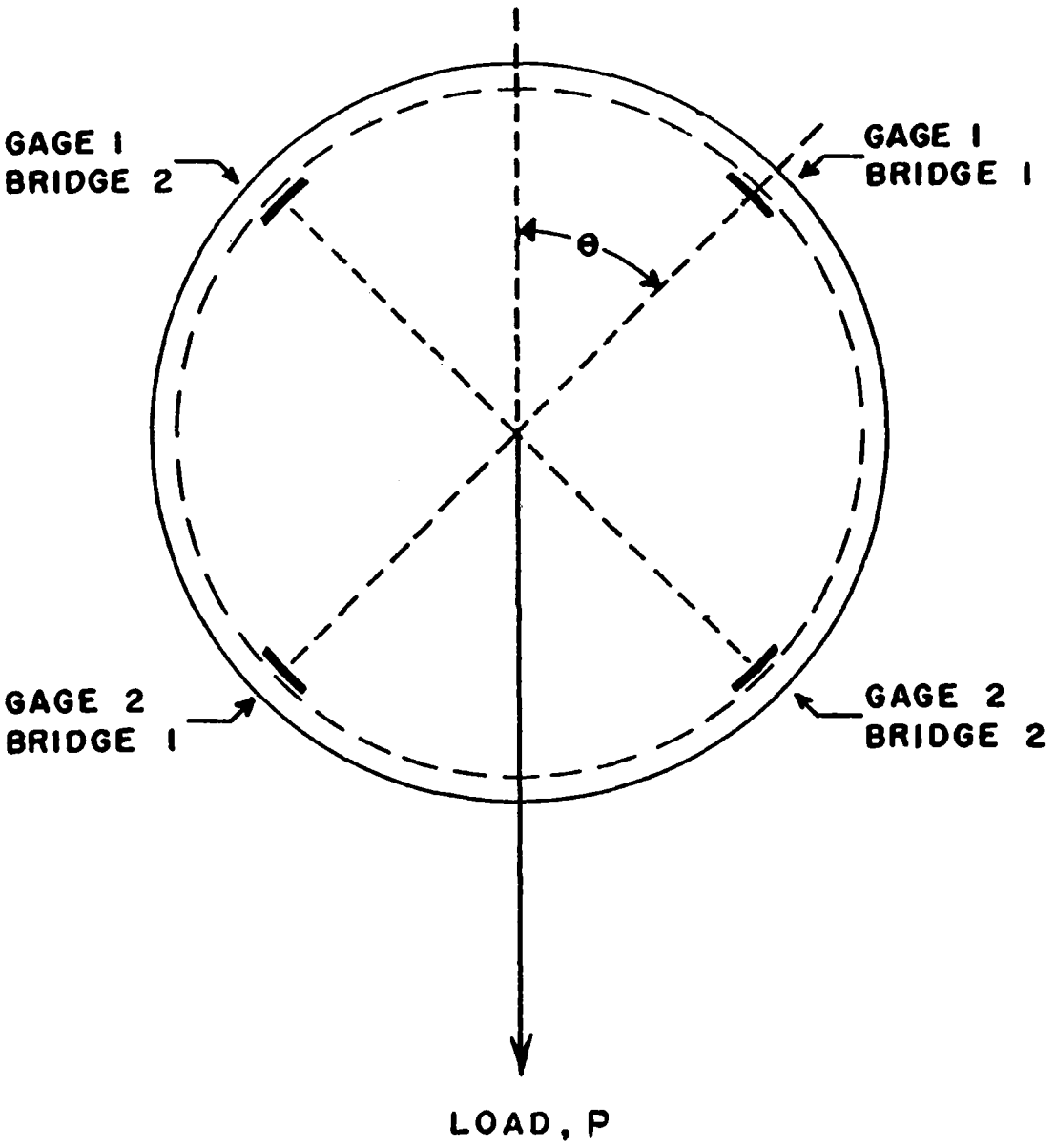

Figure 8. Schematic of transverse load P and strain gage locations for static calibration.

$$\varepsilon = h \frac{d^2y}{dx^2} = \frac{d_i P}{2EI} (\ell - x). \quad (35)$$

At the base of the beam and in terms of the component of P acting at the strain gage location, the bending strain is

$$\varepsilon = \frac{d_i P \cos \theta \ \ell}{2EI} \quad (36)$$

The data obtained in the static calibration will be compared with values computed using equation (36).

The data will be examined to determine the angular resolution, symmetry of response, linearity and hysteresis of the gage.

7.2 SHOCK TUBE TESTS.

In calibrating the flow direction gage versus incident angle of flow, only flows incident in the forward hemisphere aligned with the gage and support shaft are considered. Flows not incident in this hemisphere will be obstructed by the support shaft for the cantilever beam.

Figure 9 shows the proposed incident angles in the vertical plane containing the vertical beam axis and support shaft. The angular interval is 22.5 degrees, and the total number of incident angles for testing is nine. Figure 10 shows the four planes in which the incident flow is to be varied. Mapping of gage response in the forward hemisphere requires 36 tests.

The first test series is to be conducted in the 0.6 m air driven shock tube at the Ballistic Research Laboratory (BRL), Aberdeen P oving Ground, Maryland. A step shock of 172 kPa (25 psi) or the maximum allowed will be used for all tests. The dynamic response characteristics of the gage will be determined, and filtering requirements investigated. The data will be analyzed to determine angular resolution and symmetry of response.

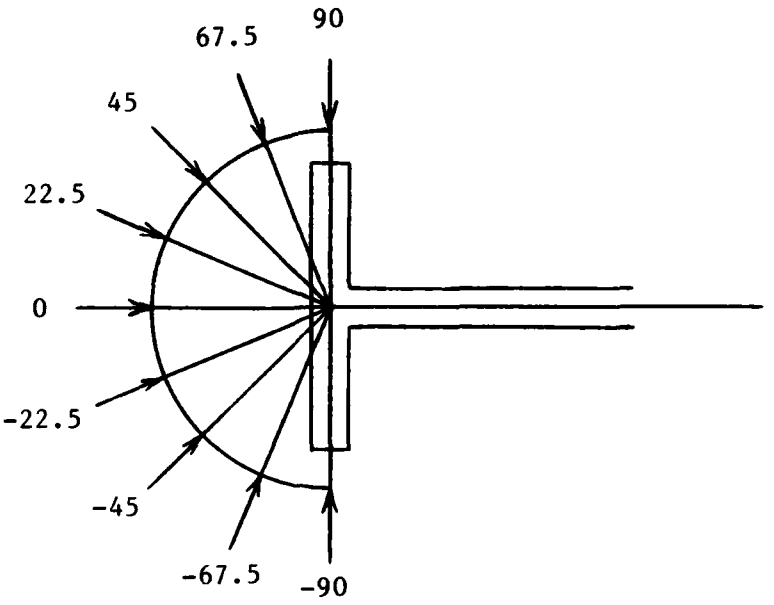

Figure 9. Flow angles for calibration in the vertical plane containing the vertical beam axis and probe support.

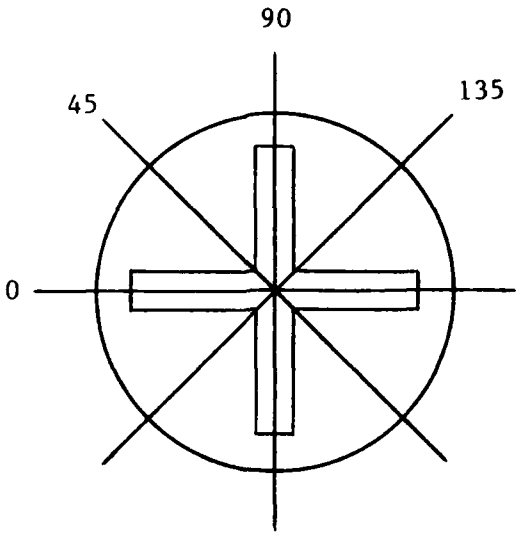

Figure 10. Planes at 0, 45, 90, and 135 degrees in which flow incident angles are to be varied for calibration.

After these initial tests and the wind tunnel tests are completed satisfactorily, the gage will be installed in the 0.43 m (17 in.) shock tube at TRW for a more limited test series. This shock tube can produce higher shock pressure than the BRL tube. Tests can be conducted with and without dust in the flow.

The initial test in the TRW tube will be made at the same shock pressure used in the shock tube tests in the BRL tube to check the correlation of gage response. Then tests will be conducted at 345 kPa (50 psi), 483 kPa (70 psi), and 621 kPa (90 psi). Four shots are to be fired at each pressure level. Two will be with the gage aligned with the flow with and without dust. Two will be with the gage at an off angle of 45 degrees, with and without dust. The data will be examined for differences between response with and without dust, and between pressure levels and previous test results.

The design of the TRW test series may be changed based on results of the BRL tube tests and wind tunnel tests.

7.3 WIND TUNNEL TESTS.

The tests in the BRL shock tube described above will provide gage response in a subsonic flow. Only supersonic wind tunnel testing is proposed because of the high velocity of the flows in the precursed blast wave where measurement of flow direction is of interest.

Tests are to be conducted at Mach numbers of 1.5, 2.0, and 2.5 over the full range of incident angles in the forward hemisphere shown in Figures 9 and 10. The data will be examined for angular resolution and symmetry, and compared with the data from the tests in the BRL shock tube.

SECTION 8

CONCLUSIONS

The precursor flow field contains regions with large and fast changes in flow direction relative to a fixed sensor. Examination of a numerical calculation of a precursed blast wave indicated a need for a sensor with a response time of 0.2 ms or less.

The response time for a rotating wind vane sensor is inversely proportional to the flow velocity. For what was considered to be the smallest practical size for a vane (22 mm), the response times were too slow for use in precursed blast waves.

After examining alternative means of sensing flow direction, the direction of bending of a cylindrical hollow cantilever beam protruding into the flow was selected as the best means for indicating flow direction. It was possible to design a beam with a response time short enough for use in precursor experiments. The beam is a hollow cylinder 41 mm long and 15 mm in diameter with a natural frequency of 8300 Hz. Because it is underdamped, the upper usable frequency is about 2080 Hz, with an associated rise time of 0.12 ms.

The basic cost of the cantilever beam flow direction sensor, once developed, is estimated to be $2100 for sensing in one plane, and $3700 for sensing in two perpendicular planes.

For development and certification of the sensor, static, shock tube, and wind tunnel tests will be required.

SECTION 9

LIST OF REFERENCES

1. Kuhl, A.L., Glowacki, W.J., Glaz, H.M., and Collela, P. "Simulation of Air Blast Precursors in Large Shock Tubes," Proceedings II of the Ninth International Symposium on Military Applications of Blast Simulation, MABS-9, St. Edmund Hall, Oxford, England, 23-27 September 1985.

2. Kuhl, A.L., R&D Associates, Marina del Rey, CA, private communications.

3. Wyngaard, J.C., "Cup, Propeller, Vane, and Sonic Anemometers in Turbulence Research," Annual Review of Fluid Mechanics, 1981.

4. Barna, P.S. and Crossman, Gary R., "Experimental Studies on the Aerodynamic Performance and Dynamic Response of Flow Direction Sensing Vanes," NASA Contractor Report NASA-CR-2683, National Aeronautics and Space Administration, Washington, DC, May 1976. (Note: The time response equation in the body of the report is in error.)

5. Usellon, J.C. and Shadow, T.O., "Results of Wind Tunnel Tests on a Flight Path Accelerometer at Mach Numbers from 0.2 to 3.0," AEDC-TR-71-260, Von Karman Gas Dynamics Facility, Arnold Engineering Development Center, Air Force Systems Command, Arnold Air Force Station, Tennessee, February 1972.

6. Glasstone, S. and Dolan, P., "The Effects of Nuclear Weapons," Department of Defense, 1977.

7. Colton, R.F., "Vortex Anemometers - Second Generation," ISA Transactions, Vol. 15, No. 4 (pg 343-353), 1976.

8. Krause, L.N. and Fralick, G.C., "Miniature Drag-Force Anemometer," NASA-TMX-3507, National Aeronautics and Space Administration, Washington, DC, June 1977.

9. Donelan, M.A. and Motycka, J., "Miniature Drag Sphere Velocity Probe," Review of Scientific Instruments, Vol. 49, No. 3, March 1978.

10. Reisler, R.E., Ethridge, N.H., and Giglio-tos, L., "Blast Measurements from a 50 Ton Hemispherical TNT Detonation in a Coniferous Forest (Operation DISTANT PLAIN, Event 4)," BRL Memorandum Report No. 1898, January 1968.

11. Reisler, R.E., Ethridge, N.H., and Giglio-tos, L., "Blast Measurements from the Detonation of Tower Placed 20 Tons of Spherical TNT (Operation DISTANT PLAIN, Events 1 and 1A)," BRL Memorandum Report No. 2089, February 1971.

12. Sakamoto, H. and Oiwake, S., "Fluctuating Forces on a Rectangular Prism and a Circular Cylinder Placed Vertically in a Turbulent Boundary Layer," Transactions of the ASME, Vol. 106, June 1984.

13. Johnson, O.T. and Ewing, Jr., W.O., "An Omni-Directional Gage for Measuring the Dynamic Pressure Behind a Shock Front," BRL Memorandum Report No. 1394, Ballistic Research Laboratories, Aberdeen Proving Ground, MD, March 1962.

14. Walden, A., Kulite Semiconductor Products, Inc., private communication.

15. Timoshenko, S., and MacCullough, G.H., "Elements of Strength of Materials," 2nd Edition, D. Van Nostrand Company, Inc., New York, New York, 1940.

16. Harris, C.M., and Crede, C.E., "Shock and Vibration Handbook," 2nd Edition, McGraw-Hill Book Company, New York, New York, 1976.

APPENDIX

LIST OF SYMBOLS

a = rate of change of lift coefficient C_L with respect to β evaluated at $\beta = 0$

A = projected vane area in the plane of zero angle of attack, or the projected area of a cantilever beam

AR = aspect ratio of vane

C_D = drag coefficient for cylindrical cantilever beam

C_L = lift coefficient for vane

d_i = interior diameter of hollow cylindrical beam

d_o = outside diameter of cylindrical beam

D = aerodynamic damping constant for vane

D_i = ratio of interior diameter to length for a hollow cylindrical beam

D_o = ratio of outside diameter to length for a hollow cylindrical beam

E = Young's Modulus for beam material

f_n = natural frequency of oscillations

F = aerodynamic force acting normal to vane at its center of pressure

h = distance from neutral axis of a beam

ℓ = length of beam

m = mass per unit length of beam

N = unit angle torgue acting on vane

P = concentrated transverse load at end of cantilever beam

Q = dynamic pressure of flowing air

r = distance between vane center of pressure and the rotation axis

R = radius of curvature of beam

t = time

t_R = vane response time, the time for the amplitude of the envelope of oscillations to reduce by a specified amount

$t_{R_{\frac{1}{2}}}$ = time for vane oscillations to decrease in amplitude by one-half

T_n = period of oscillations at the natural frequency

$\overline{U}$ = wind velocity vector

U = wind velocity magnitude

$\overline{U}_v$ = air velocity relative to vane

w = force per unit length along a beam

x = distance along beam

y = deflection of cantilever beam

β = angle of wind vector with respect to vane

β_o = peak amplitude of angular deviation of vane

β_R = vane oscillation amplitude at t_R

β_v = angle between air velocity vector U_v and vane, the instantaneous angle of attack

ϵ = strain in a fiber of a bent beam

ζ = damping ratio

Θ = angle describing orientation around axis of cylindrical cantilever beam

ρ = air density

ρ_m = density of beam material

ω_n = angular natural frequency

DISTRIBUTION LIST

DNA-TR-88-180

DEPARTMENT OF DEFENSE

ASSISTANT SEC OF DEF (C3I)
ATTN: ASD (C3I)

ASSISTANT TO THE SECRETARY OF DEFENSE ATOMIC ENERGY
ATTN: EXECUTIVE ASSISTANT

DEFENSE ADVANCED RSCH PROJ AGENCY
ATTN: DIR
ATTN: GSD
ATTN: PMO

DEFENSE ELECTRONIC SUPPLY CENTER
ATTN: DEFC-EAA

DEFENSE INTELLIGENCE AGENCY
ATTN: C WIEHLE
ATTN: RTS-2B

DEFENSE NUCLEAR AGENCY
ATTN: DFRA
ATTN: NASF
ATTN: NAWE
ATTN: OPNA
ATTN: OPNS
ATTN: RAAE B PRASAD
ATTN: SPSD
ATTN: SPWE/RINEHART
2 CYS ATTN: TDTR
4 CYS ATTN: TITL

DEFENSE NUCLEAR AGENCY
ATTN: NMHE
ATTN: NMHE LCDR TAYLOR
ATTN: RSTR
ATTN: TDNM-CF
ATTN: TDTT W SUMMA
ATTN: TTST

DEFENSE NUCLEAR AGENCY
ATTN: TDNV

DEFENSE TECHNICAL INFORMATION CENTER
2 CYS ATTN: DTIC/FDAB

DEPARTMENT OF DEFENSE EXPLO SAFETY BOARD
ATTN: CHAIRMAN

JOINT STRAT TGT PLANNING STAFF
ATTN: JK
ATTN: JKAD
ATTN: JKCS
ATTN: JPEP

LAWRENCE LIVERMORE NATIONAL LABORATORY
ATTN: DNA-LL

OFFICE OF THE JOINT CHIEFS OF STAFF
ATTN: GD50
ATTN: J-8/CAD

DEPARTMENT OF THE ARMY

HARRY DIAMOND LABORATORIES
ATTN: SCLHD-DTSO
ATTN: SLCHD-NW-RA
ATTN: SLCIS-IM-TL

U S ARMY ARM, MUNITIONS, AND CHEM COMMAND
ATTN: MA LIBRARY

U S ARMY ATMOSPHERIC SCIENCES LAB
ATTN: SLCAS-AE

U S ARMY BALLISTIC RESEARCH LAB
ATTN: TECH LIB
ATTN: R RALEY

U S ARMY COLD REGION RES ENGR LAB
ATTN: TECHNICAL DIRECTOR

U S ARMY COMMUNICATIONS R&D COMMAND
ATTN: L DORKIN

U S ARMY ELECTRONICS R & D COMMAND
ATTN: DELET-ER

U S ARMY ENGINEER CTR & FT BELVOIR
ATTN: ATZA-DTE-ADM
ATTN: DT-LRC

U S ARMY ENGINEER DIV HUNTSVILLE
ATTN: E WILLIAMS
ATTN: HNDED-SY

U S ARMY ENGR WATERWAYS EXPER STATION
ATTN: D OUTLAW
ATTN: TECHNICAL LIBRARY
ATTN: J K INGRAM

U S ARMY FOREIGN SCIENCE & TECH CTR
ATTN: DRXST-SD

U S ARMY MATERIEL COMMAND
ATTN: AMCCN

U S ARMY NUCLEAR & CHEMICAL AGENCY
ATTN: MONA-NU

U S ARMY NUCLEAR EFFECTS LABORATORY
ATTN: R BENSON

U S ARMY STRATEGIC DEFENSE CMD
ATTN: CSSD-H-SA
ATTN: DASD-TD

U S ARMY STRATEGIC DEFENSE COMMAND
ATTN: F HOKE
ATTN: CSSD-H-SAV

U S ARMY TANK AUTOMOTIVE R&D COMMAND
ATTN: TECH LIB

U S ARMY WHITE SANDS MISSILE RANGE
ATTN: STEWS-FE-R
ATTN: STEWS-TE-N K CUMMINGS
ATTN: STEWS-TE-N T ARELLANES

USA SURVIVABILITY MANAGMENT OFFICE
ATTN: J BRAND

DEPARTMENT OF THE NAVY

NAVAL ELECTRONICS ENGRG ACTVY, PACIFIC
ATTN: D OBRYHIM

NAVAL FACILITIES ENGINEERING COMMAND
ATTN: CODE 04B

NAVAL RESEARCH LABORATORY
ATTN: TECH LIB
ATTN: W ALI
ATTN: J DAVIS
ATTN: E FRIEBELE
ATTN: CODE 7780

NAVAL SEA SYSTEMS COMMAND
ATTN: J KUDZAL

NAVAL SURFACE WARFARE CENTER
ATTN: CODE H14
ATTN: TECH LIB

NAVAL SURFACE WARFARE CENTER
ATTN: TECHNICAL LIBRARY

NAVAL WEAPONS CENTER
ATTN: C AUSTIN
ATTN: J BOWEN
ATTN: TECH SVCS

NAVAL WEAPONS EVALUATION FACILITY
ATTN: CLASSIFIED LIBRARY

OFC OF THE DEPUTY CHIEF OF NAVAL OPS
ATTN: STRAT EVAL & ANAL BR

OFFICE OF NAVAL RESEARCH
ATTN: CODE 1132SM

SPACE & NAVAL WARFARE SYSTEMS CMD
ATTN: PME 117-21

DEPARTMENT OF THE AIR FORCE

AFIS/INT
ATTN: INT

AIR FORCE ARMAMENT LABORATORY
ATTN: J COLLINS

AIR FORCE INSTITUTE OF TECHNOLOGY/EN
ATTN: C BRIDGMAN

AIR FORCE WEAPONS LABORATORY
ATTN: NTE
ATTN: R HENNY
ATTN: NTES-G
ATTN: SUL

BALLISTIC MISSILE OFFICE
ATTN: MYE

STRATEGIC AIR COMMAND/XRFS
ATTN: XRFS

DEPARTMENT OF ENERGY

LAWRENCE LIVERMORE NATIONAL LAB
ATTN: B HUDSON

LOS ALAMOS NATIONAL LABORATORY
ATTN: C F KELLER
ATTN: M PONGRATZ
ATTN: MS P364 REPORT LIBRARY
ATTN: P WHALEN
ATTN: P B LYONS
ATTN: R BROWNLEE
ATTN: REPORT LIBRARY
ATTN: S S HECKER

SANDIA NATIONAL LABORATORIES
ATTN: J T HOLMES
ATTN: J S PHILLIPS
ATTN: J WALKER
ATTN: L ANDERSON
ATTN: C D BROYLES
ATTN: J D PLIMPTON
ATTN: B BENJAMIN
ATTN: J E BEAR
ATTN: TECH LIB 3141

OTHER GOVERNMENT

CENTRAL INTELLIGENCE AGENCY
ATTN: OSWR/NED

DEPARTMENT OF COMMERCE
ATTN: R LEVINE

FEDERAL EMERGENCY MANAGEMENT AGENCY
ATTN: J F JACOBS

DEPARTMENT OF DEFENSE CONTRACTORS

AEROSPACE CORP
ATTN: L SELZER
ATTN: LIBRARY ACQUISITION

AVCO CORPORATION
ATTN: A PALLONE
ATTN: W REINECKE

BDM CORPORATION
ATTN: LIBRARY

BDM INTERNATIONAL INC
ATTN: E DORCHAK

BOEING CO
ATTN: A LUNDE
ATTN: R J WOOD

CALIFORNIA RESEARCH & TECHNOLOGY, INC
ATTN: J THOMPSON

CARPENTER RESEARCH CORP
ATTN: H J CARPENTER

DAYTON, UNIVERSITY OF
ATTN: B WILT
ATTN: N OLSON
ATTN: R SERVAIS

GENERAL RESEARCH CORP
ATTN: R PARISSE

GEO CENTERS, INC
ATTN: E MARRAM

GEORGIA INSTITUTE OF TECHNOLOGY
ATTN: C BROWN

H & H CONSULTANTS, INC
ATTN: W HALL

IIT RESEARCH INSTITUTE
ATTN: DOCUMENTS LIBRARY

KAMAN SCIENCES CORP
ATTN: L MENTE
ATTN: LIBRARY

KAMAN SCIENCES CORP
ATTN: B KINSLOW

KAMAN SCIENCES CORP
ATTN: E CONRAD

KAMAN SCIENCES CORPORATION
ATTN: DASIAC

KAMAN SCIENCES CORPORATION
ATTN: DASIAC

KARAGOZIAN AND CASE
ATTN: J KARAGOZIAN

LOCKHEED MISSILES & SPACE CO, INC
ATTN: L CHASE
ATTN: R SMITH
ATTN: S SALISBURY
ATTN: T FISHER

LOCKHEED MISSILES & SPACE CO, INC
ATTN: TECH INFO CTR

MISSION RESEARCH CORP
ATTN: TECH LIBRARY

NICHOLS RESEARCH CORP, INC
ATTN: R BYRN

PACIFIC-SIERRA RESEARCH CORP
ATTN: H BRODE

PACIFICA TECHNOLOGY
ATTN: TECH LIBRARY

PHYSICS APPLICATIONS, INC
ATTN: DOCUMENT CONTROL

PHYSICS INTERNATIONAL CO
ATTN: J SHEA

R & D ASSOCIATES
ATTN: C K B LEE
ATTN: D SIMONS
ATTN: P RAUSCH
ATTN: T MAZZOLA
ATTN: TECHNICAL INFORMATION CENTER

RAND CORP
ATTN: B BENNETT

ROCKWELL INTERNATIONAL CORP
ATTN: L PINSON

S-CUBED
ATTN: R DUFF

SCIENCE APPLICATIONS INTL CORP
ATTN: K SITES

SCIENCE APPLICATIONS INTL CORP
ATTN: TECHNICAL LIBRARY
ATTN: W PLOWS

SCIENCE APPLICATIONS INTL CORP
ATTN: J MCRARY

SCIENCE APPLICATIONS INTL CORP
ATTN: TECHNICAL LIBRARY

SCIENCE APPLICATIONS INTL CORP
ATTN: J COCKAYNE
ATTN: R SIEVERS
ATTN: W CHADSEY
ATTN: W LAYSON

SCIENCE APPLICATIONS INTL CORP
ATTN: G BINNINGER

SRI INTERNATIONAL
ATTN: D KEOUGH
ATTN: D MCDANIEL

TECH REPS, INC
2 CYS ATTN: G WATSON
2 CYS ATTN: N ETHRIDGE

TELEDYNE BROWN ENGINEERING
ATTN: J RAVENSCRAFT
ATTN: P SHELTON

TRW INC
ATTN: J TAMBE
ATTN: TECH INFO CTR

TRW SPACE & DEFENSE SYSTEMS
ATTN: W WAMPLER